Geoderma Regional 37 (2024) e00818

Contents lists available at ScienceDirect

Geoderma Regional

journal homepage: www.elsevier.com/locate/geodrs

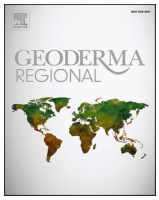

# Maintaining favourable carbon balance in boreal clay soil is challenging even under no-till and crop diversification

Henri Honkanen *, Visa Nuutinen, Jaakko Heikkinen, Riitta Lemola, Eila Turtola, Janne Kaseva, Kristiina Lång

*Natural Resources Institute Finland (Luke), Latokartanonkaari 9, FI-00790 Helsinki, Finland*

ARTICLE INFO

*Keywords:*
Soil aggregates
Earthworms
No-till
erosion
Net ecosystem exchange
Luvisols

ABSTRACT

We explored the carbon balance, including both gaseous and waterborne carbon, of a long-term experimental site in 2019 and 2020. Additionally, we assessed earthworm abundance and soil aggregation, aiming to uncover potential factors influencing the decomposition and stabilization capacity of organic carbon in the soil. The heavy clay soil site in southern Finland was under long-term cereal monocropping with conventional tillage (CT) and no-till (NT) treatments. Short-term diversification with cover crop and winter rapeseed as a break crop were applied on parts of the site, and the effects of climate, carbon input and soil conditions on the carbon balance were assessed. Net ecosystem exchange (NEE) ranged from −0.32 to 1.91 Mg $CO_2$-C $ha^{-1}$ $yr^{-1}$ in CT and from 0.22 to 2.40 Mg $CO_2$-C $ha^{-1}$ $yr^{-1}$ in NT. Net ecosystem carbon balance ranged from 1.49 to 3.27 Mg C $ha^{-1}$ $yr^{-1}$ and 1.51 to 3.67 Mg C $ha^{-1}$ $yr^{-1}$ in CT and NT, respectively, indicating carbon loss from soil. The differences in NEE or carbon balance between CT and NT were not statistically discernible. Earthworm abundance was higher in NT than in CT and increased vastly in the NT management after diversification of the rotation with winter rapeseed. Soil erosion measurements showed remarkably lower carbon loss (44%) for NT compared to CT, however, the role of erosion in the carbon balance was minor, ranging from 50 to 120 kg C $ha^{-1}$ $yr^{-1}$. The mean size of soil aggregates decreased during the study period, and soil aggregates tended to enlarge in the summer and diminish in the winter. The results highlight the difficulty of maintaining a positive carbon balance in boreal agricultural soils with limited productivity. Furthermore, future climatic conditions may worsen the situation by promoting decomposition and restricting carbon protection in soil aggregates.

## 1. Introduction

Soil organic carbon (SOC) has a significant role both in climate change mitigation and securing food production (Minasny et al., 2017; Manns and Martin, 2018). Globally, the majority of terrestrial organic carbon is stored in soil, and land use and management greatly affect the size and function of the carbon stocks (Scharlemann et al., 2014). Intensive land management decreases the carbon content of agricultural soils globally (Olsson et al., 2019) and such trend has been documented also in the boreal region (Heikkinen et al., 2022). Soil conserving, regenerative management with no-till and diversification of crop rotations can potentially improve the soil carbon balance and other ecosystem services provided by croplands (Kremen and Miles, 2012).

In no-till (NT) management, seeds are sown directly to the stubble whereas in conventional tillage (CT) the soil is annually ploughed and harrowed before sowing annual crops. NT has been found to increase the SOC content in the topsoil but decrease it in the deeper layers compared to CT in which the crop residue-derived carbon is mixed deeper and more evenly into the plough layer (Haddaway et al., 2017; Meurer et al., 2018; Ogle et al., 2019).

Soil physical fractions are sensitive to soil management changes in short-term and thus soil aggregate size distribution can be beneficial tool in soil carbon studies (Amézketa, 1999). The size distribution is often related to stabilization of carbon stocks, macrofaunal density and erosion resistance (Briones and Schmidt, 2017). NT improves soil aggregation and reduces erosion (Wang et al., 2019; Honkanen et al., 2021) but may decrease yields thereby limiting its potential to increase SOC via carbon input in crop residue (Ogle et al., 2012). Soil biological activity has been found to increase under NT management compared to CT (Kladivko et al., 1997; Green et al., 2007). This has two contrasting implications related to enhanced earthworm activity in NT soil: increased potential to stabilize carbon into soil aggregates and the

* Corresponding author.
*E-mail address:* henri.m.honkanen@luke.fi (H. Honkanen).

https://doi.org/10.1016/j.geodrs.2024.e00818
Received 9 February 2024; Received in revised form 23 May 2024; Accepted 23 May 2024
Available online 24 May 2024

higher decomposition rates of soil organic matter (Lubbers et al., 2015; Briones and Schmidt, 2017; Sheehy et al., 2019). NT is an applicable method also in northern regions, but cold boreal conditions pose a risk to aggregate stability. Long winter period with freeze and thaw cycles leads to aggregate breakdown which diminishes soil conservation potential via management practices improving soil aggregation (Le Guillou et al., 2012; Edwards, 2013; Bottinelli et al., 2017).

Diverse crop rotations have been found to improve the resilience of cropping systems against multiple environmental stressors and benefit soil quality in terms of nutrient cycling, structure, biodiversity and SOC (Gaudin et al., 2015; Yang et al., 2019; Tamburini et al., 2020). Cereal monocultures can be broken e.g. by autumn sown oilseed crops, catch crops or cover crops, and diversity can also be achieved by inter- or multicropping. Carbon sequestration potential of cover crops is estimated to be 320 kg $ha^{-1}$ $yr^{-1}$ globally (Poeplau and Don, 2015). Adopting a diverse crop rotation and conservation agriculture was found to increase carbon stocks e.g. in the United States (Nunes et al., 2018) and in India (Hazra et al., 2019; Jat et al., 2019). In boreal conditions, crop residue input from the additional biomass of cover crops or new crops in the rotation has been found to be limited (Lizarazo et al., 2020). While the benefits of diversification are apparent, it is not well known how the changes in quantity and quality of crop residues modify soil community and organic matter decomposition rate (Yan et al., 2018). Recent studies in boreal arable fields have shown that cereal monocultures can have impoverished earthworm communities compared with more diverse rotations (Hagner et al., 2023) while on set-asides the community composition can be strongly affected by the plant seed mixture used (Hyvönen et al., 2021).

Changes in SOC stocks are slow and detecting small changes in a large and spatially highly variable SOC stock by soil sampling can be difficult (Heikkinen et al., 2021a). Flux measurements provide a valuable tool to estimate the short-term carbon dioxide ($CO_2$) exchange between the atmosphere and soil surface and to understand factors driving the changes in SOC stock. Soil carbon balance depends on the carbon input from crop residues bound by plant photosynthesis and the output mostly from plant and soil respiration as well as export of carbon in the crop yield and soil erosion. Annual cropping has a lower potential than grasslands to maintain the SOC stocks as was found in a long-term monitoring of Finnish croplands (Heikkinen et al., 2013) and in a long-term experiment (Begum et al., 2022). In Finnish cultivated mineral soils, a few full-year carbon balance measurements have been done on grasslands but none in cereal production. The carbon balance of Finnish grasslands has shown net sequestration during a measurement period that did not include the sward renewal which is in most cases needed every 3–4 years in the boreal climatic conditions (Lind et al., 2016; Heimsch et al., 2021). However, these estimates did not include the carbon removed with erosion, and these different routes are generally very rarely studied simultaneously. Erosion rates can be quite large, as Honkanen et al., 2021 observed, but the amount of organic matter in erosion may still be small (Manninen et al., 2023) in relation to soil respiration.

The objective of this study was to understand the factors regulating the carbon balance of a typical annual cropping system of cereal crops in boreal conditions. For this purpose, carbon flux measurements together with continuous erosion measurements were set up at a clay soil site in southern Finland. We hypothesized that 1) the majority of the organic carbon loss from the field occurs through soil respiration while lateral transport through water runoff has a minor role, 2) soil macrofaunal abundance and diversity benefit from NT and crop diversification practices and 3) soil aggregate breakdown during the winter counteracts aggregate formation and growth during the summer in boreal climate.

## 2. Methods

### 2.1. The study site

The study site was located in Kotkanoja, Jokioinen, in southwestern Finland (60° 49′ N, 23° 30′ E, about 100 m a.s.l. slope 1–4% (mean 2%)). The climate is boreal humid with a long-term (1991–2021) annual mean temperature of 5.2 °C, total annual precipitation of 621 mm, global radiation of 3358 MJ $m^{-2}$ and sunshine duration of 1699 h (Jokinen et al., 2021). Typically, the soil is frozen and has snow cover from December to March. The average contents of clay, silt and sand in the topsoil (0–30 cm) are 60, 16 and 24%, respectively and the soil is classified as Protovertic Luvisol. Dry bulk density in the topsoil (0–10 cm) was 1.15 ± 0.07 g $cm^{-3}$ ($n$ = 8) in CT managed plots and 1.21 ± 0.07 g $cm^{-3}$ (n = 8) in NT managed plots in spring 2018 (Honkanen et al., 2021) and pH was 6.2 on average (Fritze et al., 2024). The experimental field was established in 1976 to study nutrient leaching and it consists of four hydrologically isolated plots with separate surface runoff collection. These four plots are each further divided into four subplots with separate subsurface drainage systems, yielding 16 subplots. Field design is described in detail in Turtola and Paajanen (1995) and Uusitalo et al. (2018).

The plots were named as A, B, C and D (Table 1 and Fig. 1). Since 2008, plots A and C were continuously under autumn mouldboard ploughing (CT) while plots B and D were under no-till (NT) management for 10 years until 2018. Spring cereals (barley (*Hordeum vulgare*), wheat (*Triticum aestivum*) and oats (*Avena sativa*)) were grown in all plots during that period. In 2018 when this experiment began, diversification options were implemented at three of the plots (A, C and D) while at plot B (NT) monocropping of cereals (barley) continued throughout the experiment. In plot A (CT), Italian ryegrass (*Lolium multiflorum*) was

**Table 1**
The crops, treatments and management by plot.

| Year | Day | A | B | C | D |
|---|---|---|---|---|---|
| **2008–2018** | | **CT** Spring cereals | **NT** Spring cereals | **CT** Spring cereals | **NT** Spring cereals |
| **2018** | | **CT + CC** Sowing Barley + ryegrass | **NT** Sowing Barley | **CT + summer ploughing** Sowing Barley Barley to silage + ploughing Sowing winter rapeseed | **NT + summer ploughing** Sowing Barley Barley to silage + ploughing Sowing winter rapeseed |
| | 23.5. | | | | |
| | 17.7. | | | | |
| | 18.7. | | | | |
| | 4.9. | Harvesting | Harvesting | | |
| | 19.10. | Ploughing | | | |
| **2019** | | **CT + CC** | **NT** | **CT** Fertilising winter rapeseed | **NT** Fertilising winter rapeseed |
| | 3.5. | | | | |
| | 10.5. | Sowing Barley + ryegrass | | | |
| | 20.5. | | Sowing Barley | | |
| | 22.8. | | | Harvesting | Harvesting |
| | 18.9. | Harvesting | Harvesting | | |
| | 30.10. | Ploughing | | Ploughing | |
| **2020** | | **CT + CC** Sowing Barley + ryegrass | **NT** Sowing Barley | **CT** Sowing Barley | **NT** Sowing Barley |
| | 1.6. | | | | |
| | 18.9. | Harvesting | Harvesting | Harvesting | Harvesting |
| | 27.10. | Ploughing | | Ploughing | |

CT = conventional tillage, NT = no-till, CC = catch crop.

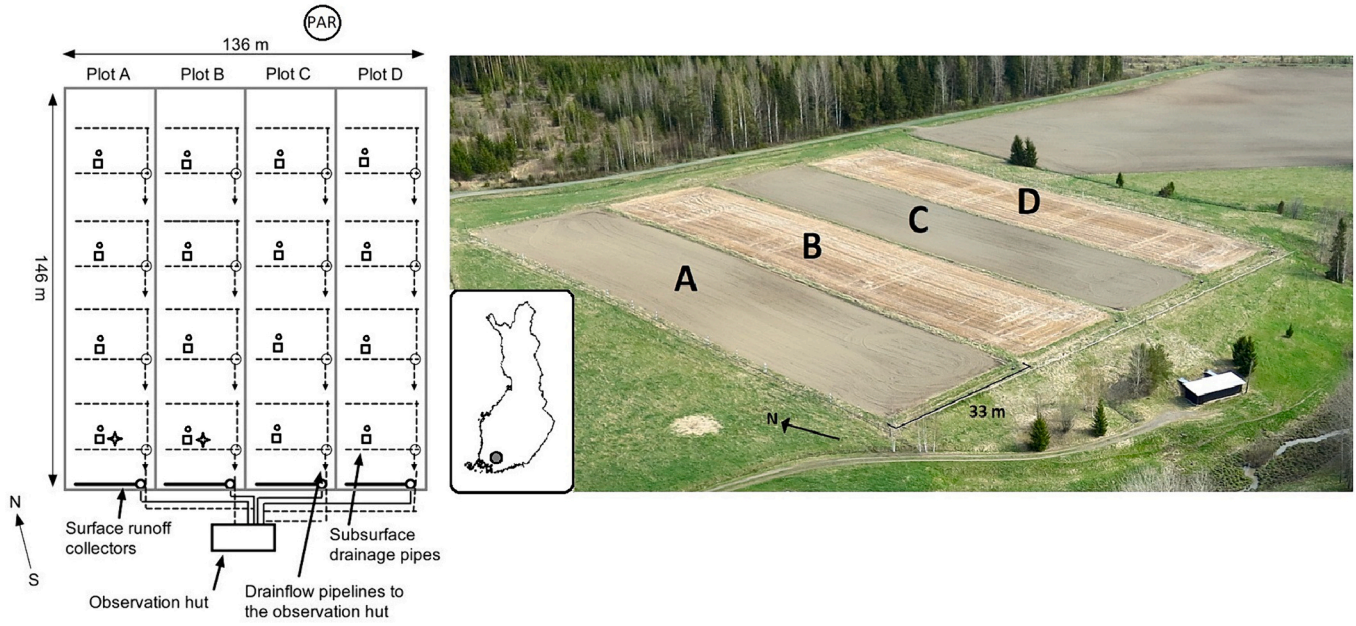


**Fig. 1.** Experimental field layout and location in Finland. Plots A and C were conventional tillage plots as well as B and D no-till plots. Chamber collars are marked with squares and bare soil chambers with circles. Stars denote the location of soil temperature sensors and PAR the location of the PAR-sensor. Figure of the field design is modified from Uusitalo et al. (2018).

added as a catch crop to barley cropping. In July 2018, when spring barley was at the early stage of growth, plots C and D were harvested for forage. After that, both plots C and D were ploughed and sown with winter rapeseed (*Brassica napus* subsp. *oleifera)* due to arrangement of another project on the same field. After this, plot D returned to NT management in 2019.

Sowing density of barley was 229 kg ha$^{-1}$ in 2018, 185 kg ha$^{-1}$ in 2019 and 269 kg ha$^{-1}$ in 2020. Each year the target was 500 germinating seeds m$^{-2}$. Ryegrass sowing density was 10 kg ha$^{-1}$ in all years and rapeseed sowing density was 4.2 kg ha$^{-1}$. Mineral NPK fertilisers (Yara Mila Y3, Yara Suomi Oy, Finland, 90–12–31 kg ha$^{-1}$ yr$^{-1}$) at sowing were used. In addition, winter rapeseed was fertilised with Yara Mila Y3 (NPK = 50–14–29 kg ha$^{-1}$) in July 2018 and with Yara Bela Suomensalpietari (110 kg N ha$^{-1}$) in May 2019. Typical farm machinery was used for cultivation. Ploughing was done to a depth of approximately 20 cm and NT sown with VM300SK (manufactured by Vieskan Metalli Oy, Finland) during the experimental period (2018–2020). Herbicides were applied to all plots in 28.6.2018 (Premium Classic SX, FMC Agricultural Solutions A/S, USA, 8 g ha$^{-1}$, Starane 333HL, Corteva Agriscience, USA, 0.3 l ha$^{-1}$). Glyphosate (Ranger XL, Monsanto Company Inc. USA, 3 l ha$^{-1}$) was applied on plots A and B in 7.5.2019 and pesticide (Decis, Bayer CropScience, Germany, 0.1 l ha$^{-1}$) on plots C and D in 11.6.2019. Also herbicides (Premium Classic SX 8 g ha$^{-1}$, Starane 333HL 0.3 l ha$^{-1}$) were applied on plots A and B in 17.6.2019. In 15.5.2020, glyphosate (Glyfomax, Dow AgroScience, USA, 3 l ha$^{-1}$) was applied on plots A and B and herbicide Ariane S, Corteva, Inc. USA, 2 l ha$^{-1}$ was applied on all plots in 30.6.2020.

Dry grain yield was measured annually with combine harvester. Above ground biomass was manually measured in two locations of each subplot from 0.5 m$^2$ area by cutting at soil surface level and weighed to estimate mass of the stubble residue. The biomass of roots was calculated using the root to shoot ratios as described in Palosuo et al. (2015). The carbon content of the crop yield, seeds and residues was assumed to be 45% (Jensen et al., 2005).

### 2.2. Ancillary measurements

Photosynthetically active radiation (PAR) was continuously measured at the edge of the field by LI-190 quantum PAR sensor (LI-COR, Lincoln, Nebraska, USA) with a one-minute sampling rate. Soil temperature was measured in A and B plots at the depth of 10 cm until May 2020 and thereafter at the depth of 5 cm to achieve better response of $CO_2$ to air temperature with Elcolog sensors (Elcoplast Oy, Tampere, Finland). Two sensors were installed in both plots with a sampling rate of one hour in summer and 2.5 h in winter. The air temperature, precipitation and global radiation data were obtained from the weather station of Finnish Meteorological Institute (FMI, CC BY 4.0) located less than a kilometre from the site. Gaps in the measured PAR data were filled with global radiation data from FMI using the ratio of global radiation and the measured PAR.

Leaf area index (LAI) was measured at the same time with the transparent chamber measurements with a portable LAI meter (SunScan; Delta-T Devices Ltd., Cambridge, United Kingdom). Because the measured LAI corresponds poorly to the actual photosynthetically active biomass in the late growing season due to the ripening of cereals, we selected the highest measured LAI values for the beginning of August and assumed that LAI is zero in the mid-September a week before harvesting when the measured gross photosynthesis (GP) was negligible. LAI between these days was interpolated. Because it was not possible to measure the LAI of the cover crop beneath the ripening barley, it was modelled based on the values of GP at PAR = 1000 μmol photon m$^{-2}$ s$^{-1}$. LAI of the cover crop in the CT plots was set to zero after ploughing.

### 2.3. Soil and earthworm sampling and analyses

Soil samples for mean weight diameter of aggregates (MWD) and carbon content were taken from the 0–10 cm and 10–30 cm soil layers in spring 2018, autumn 2018, autumn 2019, autumn 2020 and in spring 2021 (only 0–10 cm layer). About 20 subsamples were taken with soil corer (3 cm in diameter) in each subplot. Then the subsamples were pooled to composite samples, nine per each four plots A, B, C and D. Part of the sample was air dried and sieved through 2 mm mesh size sieve for carbon analyses while rest of the sample for MWD was stored at 8 °C before sieving through an 8 mm sieve and air drying.

The carbon content of the air dried and sieved (2 mm) soil samples was determined using dry combustion (LECO TruMac CN, LECO

corporation, MI).

The MWD was determined by wet sieving. For that, 50 g of the air-dried soil sample (8 mm) was fractionated into large macroaggregates (> 2 mm), small macroaggregates (0.250–2 mm) and microaggregates (0.053–0.25 mm) (Elliott 1986). The residual amount of silt and clay (< 0.053 mm) was estimated by weighing (2020 and 2021 samples) or subtracting the other fractions from the original sample (2018 samples). The MWD was calculated as in Van Bavel (1950).

Earthworm abundance and species diversity were measured in each of the 16 subplots in Oct 2018 and Oct 2020 when earthworms were active in the topsoil. Three samples were taken from each subplot by combined hand-sorting and mustard oil (AITC) extraction (ISO 23611-1:2018). Details of the earthworm sampling and measurements are described in Nuutinen (2019) and Honkanen et al. (2021).

### 2.4. Flux measurements

The $CO_2$ fluxes were measured using four different methods: opaque chambers, transparent chambers, snow gradient method and small soil respiration chambers. Between 6/2018–12/2020, closed opaque chambers were used to measure ecosystem respiration. In this study, results from plots A and B in 2019 and plots A–D in 2020 are presented for full annual budgets. In each subplot a 60 cm × 60 cm aluminium collar was installed five metres from the subsurface drain trenches (Fig. 1) to an approximate depth of 5–10 cm. An aluminium chamber (height 40 cm) mounted at the top of the collar was sealed with water in the groove of the upper edge of the collar. Steel extensions (20 or 40 cm) were used when the height of the crop exceeded the height of the chamber. The collars were removed before and reinstalled after sowing, harvesting and ploughing. The measurements were done during daytime between 10 am and 2 pm every two weeks in growing season, and every month in the winter. The chambers were closed for 30 min, and four gas samples were taken with a syringe to pre-vacuumized vials (Exetainer, Labco, UK) in 10-min intervals starting immediately after closing. Prior to sampling, the syringe was pumped a few times to mix the air in the chamber. The samples were analysed with a gas chromatograph equipped with a flame ionizer detector (FID) and a nickel catalyst for converting $CO_2$ to $CH_4$. The precolumn and analytical columns consisted of 1.8 and 3 m long steel columns, respectively, packed with 80/100 mesh Hayesep Q (Supelco Inc., Bellefonte, PA, USA). The gas chromatograph (Agilent 7890 Agilent Technologies, Inc., Wilmington, DE, USA) had a 10-way valve with a 2 ml sample loop and a backflush system for separating water from the sample and flushing the precolumn between the runs. Nitrogen was used as the carrier gas and a standard gas mixture of known concentration of $CO_2$ was used for calibration. An autosampler (222 XL Liquid handler, Gilson Medical Electronics, France) fed the samples to the loop of the gas chromatograph. A linear regression model was fitted to convert areas produced by gas chromatograph to gas concentrations. The $CO_2$ flux for each enclosure was calculated using the ideal gas law, assuming a linear change in $CO_2$ concentration over time within the chamber.

A transparent chamber (60 × 60 × 60 cm) made of polycarbonate plexiglass (1 mm, light transmission 95%) was used to measure net ecosystem exchange (NEE) approximately biweekly during the growing season. The chamber was equipped with a Vaisala GMP-343 probe and a temperature and humidity sensor (Vaisala Oy, Vantaa, Finland) and two fans for mixing the air during the measurement. One or two layers of a white fabric shroud and one blackout curtain were used to control the amount of light entering the chamber (approximately 100%, 50%, 25%, 0% of ambient radiation). The measurements were done in the same collars as the opaque chamber measurements. Four measurements with different levels of entering light were taken from each subplot in order to cover a large range of light conditions during one measurement round. Each measurement took one minute with a five second sampling rate. The chamber was flushed after each measurement to reconstitute ambient $CO_2$ and air humidity contents. A lag time of 10 s was applied after closing and before starting the measurement to exclude the dead-band when the flux was not yet stabilized. Clear sky conditions were preferred to avoid problems related with changing cloud cover and to achieve the widest possible range of available light. On the hottest summer days, freezer blocks were used to cool the chamber air. The temperature change inside the chamber was <1.5 °C which was also used as a criterion for data filtering.

The change of $CO_2$ concentration during the chamber enclosure was assumed to be linear. The measurement results of $CO_2$ as parts per million (ppm) unit were converted to g $m^{-2}$ $h^{-1}$ by the ideal gas law using measured temperature inside the chamber.

If the depth of snow cover was >20 cm, a concentration snow gradient method as in Maljanen et al. (2003) was used to determine the GHG fluxes. A probe made of a steel pipe (Ø 3 mm), with a three-way valve and a plastic syringe, was used to sample 15 ml of air just above the snow cover, in the bottom of the snow cover and at one depth in between in three replicates per plot (intermediate depth depended on the snow depth). The gas was stored in the pre-vacuumized vials and the concentrations were determined gas chromatographically as with the opaque chamber samples. The fluxes were calculated using the equation based on Fick's law as in Maljanen et al. (2003).

Measurements for bare soil respiration were made in 7/2019–12/2020. One steel air ventilation pipe of 27 cm in diameter and 30 cm in length was installed to the depth of 5–10 cm in each of the 16 subplots next to the opaque chamber collars (Fig. 1). All green vegetation within the chamber area was removed. For the measurements, the cylinders were closed with a cover equipped with a $CO_2$ sensor (GMP-343; Vaisala Oyj, Vantaa, Finland) and a small fan. One measurement lasted for one minute with a five second sampling rate. Measurements were done once in a week or two weeks, more frequently in summer than in winter. Measurements were used to estimate the total soil respiration in the growing seasons of 2019 and 2020.

### 2.5. Flux modelling

NEE (net ecosystem exchange) consists of GP (gross photosynthesis) and ER (ecosystem respiration) and thus GP (g $CO_2$ $m^{-2}$ $h^{-1}$) was estimated for each NEE measurement by (Eq. (1)),

$$GP = NEE - ER \quad (1)$$

where the full darkened transparent chamber measurement result, ER (g $CO_2$ $m^{-2}$ $h^{-1}$), is subtracted from the light-dependent flux, NEE (g $CO_2$ $m^{-2}$ $h^{-1}$), measured during the same day. Thus, we follow the sign convention with positive ER and negative GP values. The light response of GP was estimated for individual plots and measurement days (four measurements per plot at 0%, 25%, 50% and 100% of ambient PAR) with a rectangular hyperbolic saturation curve (Thornley and Johnson, 1990):

$$GP = \frac{\alpha^{*}\mathrm{PAR}^{*}GP_{max}}{\alpha^{*}\mathrm{PAR} + GP_{max}} \quad (2)$$

where α (g $CO_2$ μmol per photons in hour) is the initial slope of the photosynthetic light response and $GP_{max}$ (g $CO_2$ $m^{-2}$ $h^{-1}$) is the maximum value of GP at infinite PAR. Estimated α and $GP_{max}$ were used to predict GP at PAR = 1000 μmol photon $m^{-2}$ $s^{-1}$ (GP1000) for individual plots and measurement days to compare differences between management methods.

Annual ER and GP (May to April) were estimated for all subplots and both years. First, unknown parameters were estimated with empirical models and measured datapoints. Model fits are shown in Table S1 and Fig. S1. After solving the unknowns, models 2–7 were fed with the timeseries of the measured environmental parameters like temperature to predict ER or GP values in the timeseries. Models were used for ER as in Lohila et al. (2003) and for GP as in Kandel et al. (2013). Instead of the phytomass indices used in the above publications, we used LAI to

describe the stage of the crop growth. Air temperature and PAR were assumed to be the same for all plots, whereas we used the measured LAI for each subplot distinctly and the soil temperature from either CT or NT plots.

We used the following equation defined by Long and Hällgren (1993) for GP (g $CO_2$ $m^{-2}$ $h^{-1}$) to estimate empirical coefficients ($A_{max}$ and k) using nonlinear regression (fitnlm function in MATLAB 2019b) based on a least-squares fit:

$$GP = \frac{A_{Max}{}^{*}PAR}{k + PAR}{}^{*}LAI{}^{*}T_{Scale} \quad (3)$$

where PAR is the measured photosynthetically active radiation, LAI is the measured leaf area index, $A_{max}$ is the asymptotic maximum (g $CO_2$ $m^{-2}$ $h^{-1}$), and k is a half-saturation value (μmol $m^{-2}$ $s^{-1}$). $T_{Scale}$ represents the temperature sensitivity of photosynthesis (0–1) and follows the equation presented by Raich et al. (1991):

$$T_{Scale} = \frac{(T - T_{min})(T - T_{max})}{(T - T_{\min})(T - T_{max}) - (T - T_{opt})^2} \quad (4)$$

where T is the measured temperature, photosynthetically active minimum temperature $T_{min}$ is −2 °C, maximum $T_{max}$ is 40 °C and the optimum is 20 °C as in (Kandel et al., 2013). Model fits are shown in Fig. S1 and Table S1.

ER consists of autotrophic ($R_{auto}$) i.e. plant respiration and heterotrophic ($R_{hetero}$) i.e. soil respiration (Lloyd and Taylor, 1994):

$$ER = R_{hetero} + R_{auto} \quad (5)$$

$$R_{hetero} = R0_s{}^{*}exp\left(E0_s\left(\frac{1}{56.02} - \frac{1}{T_{soil} + 46.02}\right)\right) \quad (6)$$

$$R_{auto} = LAI{}^{*}R0_p{}^{*}exp\left(b_d\left(\frac{1}{10 + 273} - \frac{1}{T_{air} + 273}\right)\right) \quad (7)$$

where $T_{soil}$ is the measured soil temperature (°C), $T_{air}$ is the measured air temperature (°C), $R0_s$ is soil respiration at the reference temperature 10 °C (g $CO_2$ $m^{-2}$ $h^{-1}$), $R0_p$ is plant respiration at the reference temperature at 10 °C (g $CO_2$ $m^{-2}$ $h^{-1}$), $E0_s$ is ecosystem sensitivity i.e. soil temperature dependence of soil respiration and was set to 308 and $b_d$ was the temperature dependence of plant respiration set to 5000 as in Lohila et al. (2003).

The empirical coefficients ($R0_s$ and $R0_p$) were estimated with a nonlinear regression model similarly as in the case of GP. Hourly timeseries of GP and ER were predicted with the above equations using the modelled parameters and hourly timeseries of the field measurements. Hourly time points for LAI and soil temperature were acquired from the measured values by linear interpolation. Hourly averages were calculated from the measured PAR. Gaps in soil temperature during sowing, harvesting or ploughing were filled with the soil temperature model (Zheng et al., 1993) based on air temperature (correlation between soil and model temperature was $R^2 = 0.88$ in the full dataset). The NEE was calculated by subtracting the modelled GP from the modelled ER. ER was estimated using data from both opaque chambers and darkened transparent chambers. Annual fluxes were computed as integral of the hourly fluxes with a trapezoidal method (trapz function in MATLAB 2019b).

Hourly soil respiration was modelled for both treatments for the periods between sowing and harvesting in 2019 and 2020 based on all bare soil respiration measurements and timeseries of soil temperature. Procedure for flux fitting was the same as for the transparent chamber measurements but in the modelling phase only eq. 6 was used to estimate the parameter $R0_S$, and the models were built up for each subplot. Total effluxes were accounted for the growing seasons (between sowing and harvesting) of 2019 and 2020.

### 2.6. Estimating of soil carbon in water discharge

Subsurface discharge was continuously monitored with the tipping bucket method from the drainage pipes of each 16 subplots and surface runoff was measured from the 4 plots (A–D) each covering four subplots. Water samples were regularly taken to determine the total amount of erosion matter in the discharge and runoff from evaporation residue containing both solid and soluble matter. Methods of analysis are described in detail in Turtola and Paajanen (1995), Uusitalo et al. (2018) and Honkanen et al., 2021. In addition, total organic carbon content was determined from randomly selected total erosion matter samples ($n$ = 77) by dry combustion (LECO TruMac CN, LECO corporation, MI). Basic exponential function was fitted to the values of erosion matter concentration samples and analysed carbon content of erosion matter measured from plots A, C and D (Fig. S2a). In plot B erosion matter and its carbon content deviated from the other plots and thus carbon content in water discharge of plot B was simply estimated using a linear regression model (Fig. S2b). Models were used to forecast total organic carbon content of each erosion matter measurement.

Erosion matter concentration in surface discharge was measured but samples were not taken to carbon analysis. Amount of carbon in surface water discharge was estimated by using the same models and parameters as for subsurface discharge. The data of Manninen et al. (2023) measured in 2015–2017 from the same experimental field showed rather similar carbon contents of the eroded soil particles both in surface and subsurface discharge. In this study, wind erosion was not accounted.

### 2.7. Carbon balance

Depending on the relationship between the carbon bound by the plant (GP) and the carbon released by the plant and soil respiration (ER), the NEE can be either positive (output) or negative (input). Additional carbon outputs are the biomass removed from the field in harvest and erosion. Erosion can result from water or wind, but wind erosion is assumed negligible in this study. Additional carbon inputs may be carbon in seeds, fertilisers or other organic amendments and by deposition of eroded material but those were not used (organic fertilisers or amendments) or are assumed negligible (deposition of eroded material) in this study. Eq. 8 defines the components in carbon balance (Mg C $ha^{-1}$ $yr^{-1}$) which were taken into account in this study.

$$Carbon\ balance = NEE + Yield + Erosion - Seeds \quad (8)$$

Negative (−) sign indicates carbon input to the field and positive (+) sign carbon output i.e. carbon loss from the field.

### 2.8. Data processing and analysis

In the flux measurements some outliers were identified at the beginning of the measurement if the flux was not yet stabilized due to fluctuations or slow response of the measuring device. Obvious outliers from the beginning (first three data points) of the transparent chamber flux measurement were removed with Matlab's "isoutlier" command. The outlier was defined to be more than three scaled median absolute deviations (MAD) from the median of the linear regression standardised residuals, and this resulted in the removal of 67 data points out of 10,700 in 855 flux measurements. For the transparent chamber measurements, the criteria $R^2 > 0.9$ for the fitted linear assumption of flux measurements would exclude a large amount of data, especially with a small change in $CO_2$, leading to a biased dataset. Therefore, we decided to add the criterion $S_{xy} < 1.5$ g $m^{-2}$ $h^{-1}$ as in Kutzbach et al. (2007) ($S_{xy}$ is the standard deviation of the residuals and 1.5 g $m^{-2}$ $h^{-1}$ is the 95% percentile of measurements). This procedure resulted in the removal of 71 values out of a total of 855 measurements. In the modelling phase, fitted values were examined, and outliers were removed to avoid distortion. Outliers were defined as observations with an absolute value of standardised residuals greater than three. In 2019, 4 out of 268 GP

values and 3 of 200 ER values were removed. In the dataset of 2020, 7 out of 512 GP values and 13 of 475 ER values were removed. The model's estimated parameters $A_{max}$, k of GP, R0s and R0p of ER and model correlations are shown in Table S1. The measured versus model predicted values of GP and ER are shown by managements and years in Fig. S1.

For the bare soil fluxes, the criterion $R > 0.9$ and $S_{xy} < 1.7$ g m$^{-2}$ h$^{-1}$ (95% of residuals) were used for data cleaning which resulted in the removal of 13 values out of 568. Outliers ($n = 17$) in the models were processed by removing measurements whose standardised residuals exceeded the threshold value of 3. The model estimated parameters are shown in Table S2.

For opaque chamber measurements, data points that did not pass the criterion $R^2 > 0.9$ (22 out of a total of 440 datapoints), were removed. All the data cleaning and processing was done with Matlab (The Math Works, Inc., MATLAB, version 2019b).

### 2.9. Statistical analyses

To analyse the effects of plot (A, B, C and D), year (2019 and 2020), and their interaction on ten response variables, we used generalized linear mixed models (GLMM) with different distributional assumptions and link functions. The assumption of a gamma distribution (with a log link) was used for soil respiration in summer, carbon in crop yield and subsurface erosion carbon, whereas other skewed response variables (ER summer, ER winter and residues carbon) were analysed using the assumption of a lognormal distribution (with an identity link). The assumption of a Gaussian distribution (with an identity link) was used for others (GP, ER, NEE and carbon balance). We estimated the model parameters using the residual pseudo-likelihood (RSPL) method for the gamma-distributed variables and the residual maximum likelihood (REML) method for the other variables.

Block (horizontal row in the field as in Fig. 1) and block × year were assumed to be independent and normally distributed random effects. Akaike's Information Criterion ($AIC_c$) was used to select the most suitable covariance structure for the experimental years. A heterogeneous compound symmetry ($CS_H$) covariance structure was used when the variances differed between years, and a homogeneous CS with constant variance otherwise. The Kenward-Roger method was used for the calculation of degrees of freedom. The Tukey-Kramer method was used for pairwise comparisons of means with a significance level of 0.05. The normality of the residuals of the models was checked using boxplots and found to be adequate.

A similar GLMM model was used for mean weight diameter (MWD) using the assumption of a Gaussian distribution and a CS covariance structure between the four time points (5/2018–5/2021). All analyses were conducted using the GLIMMIX procedure in the SAS Enterprise Guide 8.3 (SAS Institute Inc., Cary, NC, USA).

In addition, we tested the relation between the earthworm density and ecosystem respiration with Pearson correlation test. We chose the opaque chamber measurements for comparison, which were made as close as possible to the observation of the earthworms in both 2018 and 2020 ($n = 32$).

## 3. Results

### 3.1. Weather conditions

Mean annual air temperature was 5.9 °C in 2019 and 7.3 °C in 2020, and precipitation was 670 mm in 2019 and 730 mm in 2020. Both mean temperature and precipitation were thus higher during the study period than during the reference period 1991–2020 when the mean temperature was 5.2 ± 0.9 °C and precipitation 621 ± 85 mm (Jokinen et al., 2021). Mean temperature in 2020 was the highest in the 30-year reference period. In 2019, precipitation was even throughout the growing season but in 2020 the dry June was followed by a period of intensive rainfall. July, the most important time for crop growth, was cloudier (sum of total radiation 150 kWh m$^{-2}$) in 2020 than in the previous year (sum of total radiation 176 kWh m$^{-2}$). Wintertime (Nov – Mar) was exceptionally warm in 2019–2020 when the mean air temperature was 0.8 °C compared to the 10-year average, −2.9 ± 2.0 °C in Honkanen et al. (2021). In both winter 2018–2019 and 2020–2021, the mean air temperature was −1.9 °C. There were 108, 13 and 81 whole days with snow cover in the three consecutive winters, respectively. In winter 2019–2020, there was no continuous snow cover whereas the snow cover was continuous from 20-Dec-2018 to 30-Mar-2019 and from 3-Jan-2021 to 24-Mar-2021.

### 3.2. $CO_2$ fluxes

Plant growth occurred during the summer with the exception of the ryegrass cover crop showing some photosynthesis and low GP values also outside the summer months (Fig. S3 and Fig. 2d). There were no large differences in GP1000 between plots during the experiment (Fig. S3). Due to earlier sowing, plot A had slightly higher GP1000 during the early stage of growth and slightly lower during the late stage of growth compared to plot B in 2019. The growth peaked during the mid-July in all plots and both years. Subplot-specific maximum value varied from 2.16 to 7.75 g $CO_2$ m$^{-2}$ h$^{-1}$. The predicted GP was primarily influenced by PAR and LAI, with temperature playing a comparatively minor role. Diurnal variation was large due to PAR varying with solar angle and cloudiness.

Measured ER did not vary significantly between treatments (Fig. S4), and its temporal variation mostly followed soil temperature (Fig. 2a) and LAI (Fig. 2c). In the late growing season, plot B showed higher ER on average as compared to plot A in 2019, and plots B and D showed higher averages compared to A and C in 2020. Model-predicted ER (Fig. 2e) followed well the temporal variation of the opaque chamber measurements (Fig. S4), featuring the highest values during the summer months. Diurnal variation was less prominent in the modelled ER than in the modelled GP as it was only following the soil and air temperature and LAI.

The period with net uptake of C (negative NEE) was restricted to the summer months (Fig. 2f). In 2019, the number of days with negative NEE was 82 and 61 in plots A–B, respectively. In 2020, the respective numbers were 43, 42, 26 and 30.

### 3.3. Carbon balance

#### 3.3.1. Gross photosynthesis

Annual estimated GP did not vary significantly by plot or year during the experiment (Tables S3 and S4). GP tended to be on average lower in CT plots compared to NT plots, but with no statistically significant difference (Table S5; $p = 0.131$).

#### 3.3.2. Ecosystem respiration

The annual estimated ER did not differ between years or plots (Tables S3 and S4). There was also no difference in the summertime, but the ER estimated for the wintertime was higher in 2020 than in 2019 ($p = 0.003$). In the comparison of CT and NT management, CT plots had significantly ($p = 0.047$) lower estimated annual ER as well as summertime ER compared to NT (Table S5).

#### 3.3.3. Net ecosystem exchange

Estimated NEE was negative only in plot A in 2019 while the other plots were always losing carbon at an annual level (Table S4). No statistically significant differences were found in the annual NEE estimates between the plots (Table S3) although plots C and D tended to have higher NEE (higher carbon loss) than plots A and B whereas no-till plots B and D tended to have higher NEE than plots A and C. Plots A and B were sequestering carbon during the summer season 2019, as the average NEE was −1.02 Mg $CO_2$-C ha$^{-1}$ in plot A and − 0.366 in plot B,

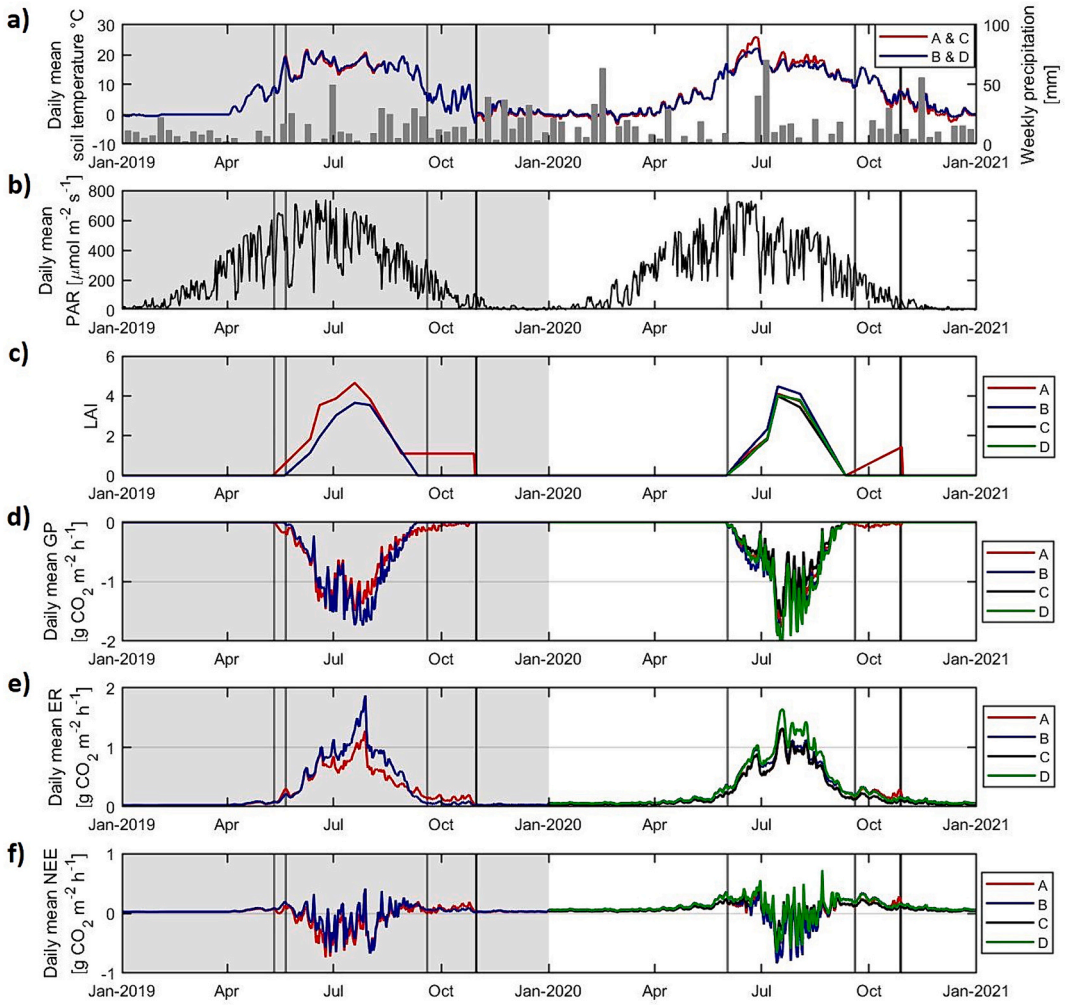


**Fig. 2.** Measured soil temperature in plots A and B and weekly precipitation (a), measured PAR during the experiment (b), measured LAI ± standard deviation (c) and daily model predicted ecosystem respiration (ER), gross photosynthesis (GP) and their sum as net ecosystem exchange (NEE) in plots A-D (d,e,f). Year 2019 is marked with grey background, sowing and harvesting the main crop with grey vertical lines and ploughing with a black vertical line.

but all plots lost carbon in 2020 with the rates of 0.040, 0.024, 0.736 and 0.628 Mg $CO_2$-C $ha^{-1}$ for plots A-D, respectively (data not shown). The years differed from each other ($p = 0.002$) indicating higher carbon losses in 2020 than in 2019. No significant difference was found in the annual estimated NEE between CT and NT treatments (Table S5).

### 3.3.4. *Bare soil respiration*

Estimated bare soil respiration during the growing season did not differ significantly by year or plots but their interaction was significant ($p = 0.033$) (Table S3). On average, soil respiration was higher in 2019 compared to 2020 but it is partly explained by a longer period between sowing and harvest (Table S4). The proportion of bare soil respiration of the total ecosystem respiration during the growing season was 79% and 89% in plots A and B in 2019 and 67%, 66%, 55% and 55 in plots A-D in 2020, respectively. The summertime soil respiration rate was significantly higher ($p = 0.015$) in NT than in CT management (Table S5).

### 3.3.5. *Yield carbon*

The amount of carbon in crop yield differed by year (p = 0.003), and there was also a statistically significant interaction of year and plot ($p < 0.001$) (Table S3). Carbon in crop yield was the highest in plot A in 2019, but there were no significant differences between the plots in 2020 (Table S4). CT and NT managements did not differ for the amount of carbon in the harvested crop yield (Table S5).

### 3.3.6. *Crop residues*

The amount of carbon in the crop residues left on the field had a similar pattern as the carbon in crop yield, with a significant ($p = 0.008$) effect for the interaction between year and plot (Table S3). Plot A had more residues in comparison to plot B in 2019 (Table S4). In 2020, no significant differences were observed between the plots or between CT and NT managements either (Table S5). In 2019, the N content of the residues varied by crop type, being 0.55 ± 0.06%, 0.41 ± 0.05% in barley plots A and B and 1.19 ± 0.20% and 1.03 ± 0.21% in the rapeseed plots C—D, respectively.

### 3.3.7. *Erosion rates*

In 2018, the total erosion rates were low, on average of 740, 280, 730, and 370 kg $ha^{-1}$ in plots A–D. In 2019, total erosion rates were larger (2940, 1280, 1530 and 1190 kg $ha^{-1}$ in plots A–D) and the largest rates were observed in 2020 (8430, 1700, 5610 and 2340 kg $ha^{-1}$ in plots A–D).

### 3.3.8. *Carbon in water discharge*

The ploughed plots A and C had the highest rates of total subsurface erosion leading to a highly significant effect ($p < 0.001$) of plot on carbon loss rates (Tables S3 and S4). The exceptional ploughing of plot D in the summer 2018 thus did not have a distinct effect on the erosion rate of the plot. Subsurface erosion carbon rates differed between years ($p = 0.001$) although erosion rates were high in winter 2019–2020 due to

mild conditions with no permanent soil frost or snow cover. CT had significantly higher ($p < 0.001$) subsurface erosion carbon rates compared to NT (Table S5) although the amount of water discharge was of the same magnitude (results not shown). Due to the higher carbon content of erosion matter in NT plots, differences in carbon in water discharge between plots were smaller compared to differences in erosion matter.

Surface erosion carbon rates were not tested statistically due to lack of replicates but on average, differences between plots tended to be smaller compared to subsurface erosion. In 2019, carbon loss in surface erosion was even higher in plot B compared to plot A. On average, the surface discharge accounted for approximately 19% of total carbon loss by erosion during this experiment.

### 3.3.9. Net ecosystem carbon balance

Total carbon balance, consisting of GP, ER, carbon in harvested yield, seeds and soil erosion, did not differ by plot but it was higher leading to greater carbon loss in 2020 compared to 2019 ($p = 0.009$; Table S3). No statistical difference was found between CT and NT management (Table S5). On average, the proportion of ecosystem respiration of the total carbon loss (total carbon balance without GP and seeds) was 80% (60% for soil respiration and 20% for crop respiration), that of carbon in crop yield 19% and carbon in erosion matter 1.3% (1.0% for subsurface erosion and 0.2% for surface erosion) (Fig. 3). The share of seeds was about 2.3% of the total carbon input, while GP was the dominant fraction.

## 3.4. Cover crop

On average, the measured mass of aboveground cover crop was 480 ± 80 kg dry matter $ha^{-1}$ in 2019 and 400 ± 210 kg dry matter $ha^{-1}$ in 2020. The estimated cover crop GP was 0.16 ± 0.06 Mg C $ha^{-1}$ in 2019 and 0.13 ± 0.02 Mg C $ha^{-1}$ from harvest to ploughing in 2020. These results are quite low compared to an estimated sum of carbon in the biomass samples and roots, yielding 0.33 ± 0.40 Mg C $ha^{-1}$ in 2019 and 0.27 ± 0.10 Mg C $ha^{-1}$ in 2020. The difference is most likely explained by the fact that the main part of the growth occurred already before the harvest of the barley.

## 3.5. Mean weight diameter of soil aggregates

MWD in the topsoil (0–10 cm) of each subplot was measured four times during this experiment (Fig. 4). During the growing season of 2018, MWD tended to increase in plots A and B and decrease in plot D that was ploughed in the midsummer (Table S6). Between autumns 2018 and 2020, no statistically significant changes were observed but plot B showed a decreasing tendency ($p = 0.095$) (Fig. 4; Table S6). During the winter of 2020–2021, MWD decreased about 19% in all plots ($p < 0.001$ for all plots). As regards the whole experimental period from spring 2018 to spring 2021, MWD decreased in plots B ($p = 0.002$) and D ($p = 0.006$). A small decrease can be seen also in plot C but in plot A the MWD even increased slightly although the changes were not statistically discernible.

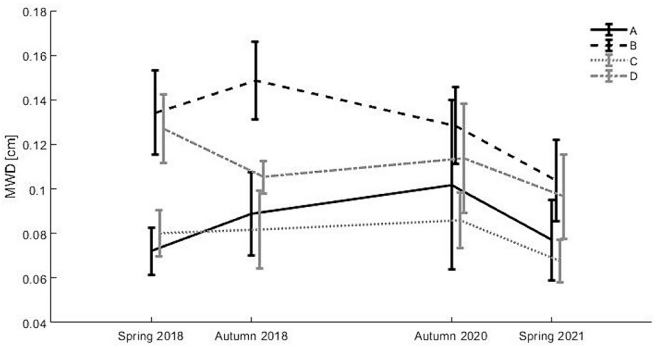


**Fig. 4.** Mean weight diameter (mean ± standard deviation) of soil aggregates in the 0–10 cm layer in plots A-D in 2018–2021.

## 3.6. Soil carbon

No statistically discernible differences in soil carbon contents were observed between plots in either layer (Fig. 5). Generally, carbon content increased during summer and decreased during winter, but the only statistically significant seasonal changes were observed during the summer of 2018. Then the carbon content in the layer 10–30 cm increased significantly in plots B ($p < 0.001$), D ($p < 0.001$) and almost significantly in plot A ($p = 0.074$). During the whole experiment, carbon content decreased on average. A statistically significant difference in the surface layer was found only in plot D where the carbon content decreased ($p = 0.004$) between May 2018 and May 2021. Due to ploughing of plot D in summer 2018, the layers were mixed, and the carbon content of the surface layer decreased while it increased in the 10–30 cm layer. Two years after the ploughing, the carbon contents of the two layers were again distinctly different and both at a lower level than at the start of the experiment. Between autumn 2018 and autumn 2020, the carbon content in the 10–30 cm layer decreased significantly in plots A ($p = 0.0194$) and D ($p = 0.0003$).

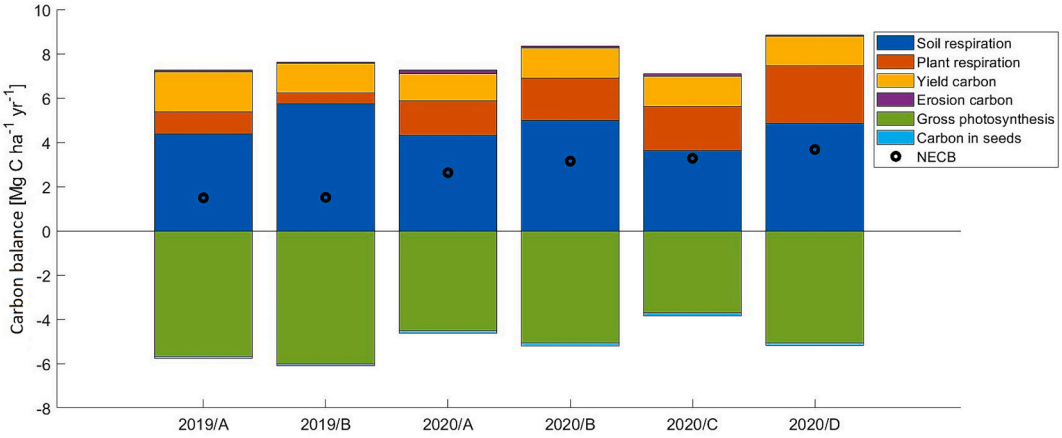


**Fig. 3.** Carbon balance and its components of plots A - D in 2019–2020. Net ecosystem carbon balance (NECB) is a sum of carbon inputs and outputs. Negative sign reflects carbon input and positive sign carbon output i.e. carbon loss from the field. All the numbers are shown in Table S4.

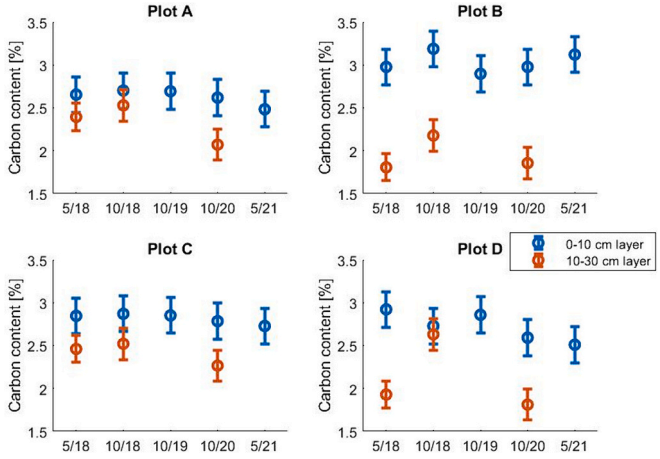


**Fig. 5.** Carbon content in two soil layers of each plot in 2018–2021.

### 3.7. Earthworms

Total abundance and species number of earthworms tended to increase in all plots from the year 2018 to 2020 (Fig. 6). The total density increased statistically significantly in all plots ($p = 0.040$, 0.041, 0.029, and $< 0.001$ in plots A, B, C and D, respectively) and the total mass in plot D ($p < 0.001$). The density of epigeic species increased significantly in plots B ($p = 0.011$) and D ($p < 0.001$), that of anecic earthworms in plot D ($p = 0.043$) and endogeic species in plots C ($p = 0.021$) and D ($p < 0.001$). In no-till plot D with rapeseed diversification, the increase of abundance was remarkably strong and much more pronounced than in the other plots. There the mean total density increased by close to 300 hundred individuals $m^{-2}$ and total mean mass by approximately 70 g $m^{-2}$, an increase of both epigeic and endogeic earthworms contributing to the population growth (Table S7). In 2020 NT plots B and D had higher earthworm total densities and masses than CT plots A and C, with NT plot D having the highest abundances. A clear qualitative difference between the earthworm communities of the treatments was the higher densities of epigeic earthworms in NT plots B and D. Anecic densities were also higher in those plots but due to large within-plot variation the differences between the treatments were not statistically significant. The number of species was two times higher in NT plots than in CT plots although the differences were not always statistically significant.

There was a strong correlation (Pearson's $r = 0.792$, $p < 0.001$) between the density of earthworms and ecosystem respiration in the temporally and spatially closest measurements. The correlation was weaker for the mass of worms (Pearson's $r = 0.480$, $p = 0.005$).

## 4. Discussion

### 4.1. Carbon balance

We present the first estimates of carbon balance based on flux measurements on mineral soil with annual cropping in Finland. Compared to published carbon balances of Finnish grasslands on mineral soil, ranging from −0.9 to 0.5 Mg C $ha^{-1}$ $yr^{-1}$ (Lind et al., 2016; Heimsch et al., 2021), our results show a much higher net carbon loss with a range from 1.5 to 3.7 Mg C $ha^{-1}$ $yr^{-1}$. The estimated carbon loss was also high compared to the average nationwide decrease of 0.2 Mg C $ha^{-1}$ $yr^{-1}$ or the decrease in cereal cropping of 0.5 Mg C $ha^{-1}$ $yr^{-1}$ based on soil monitoring of Finnish mineral croplands (Heikkinen et al., 2013; Saarinen et al., 2023). The several-fold difference between the results is striking although it is known that annual cropping typically features the highest carbon losses (Heikkinen et al., 2022). Total annual carbon losses ranged from 1% to 4% (mean 2%) of the total carbon stock of the plots in spring 2018 (Honkanen et al., 2021). The year 2020 was exceptional due to high mean temperature and almost snowless winter, which may partly explain the large carbon loss. Such conditions have earlier been recognized as one climate change related factor likely accelerating the carbon stock decline in boreal agricultural soils (Heikkinen et al., 2022). It may be challenging to increase carbon stocks with soil management practices in boreal clay soils where carbon stocks are already high and potential to stabilize carbon on mineral surfaces already largely used (Poirier et al., 2013; Soinne et al., 2024). Targeting improved management to fields and regions with the highest carbon saturation deficit is crucial for effective carbon sequestration.

Annual budget of GP was always lower or only slightly higher than ER, and the carbon export in harvest turned this balance clearly unfavourable from the viewpoint of SOC conservation. Part of the high

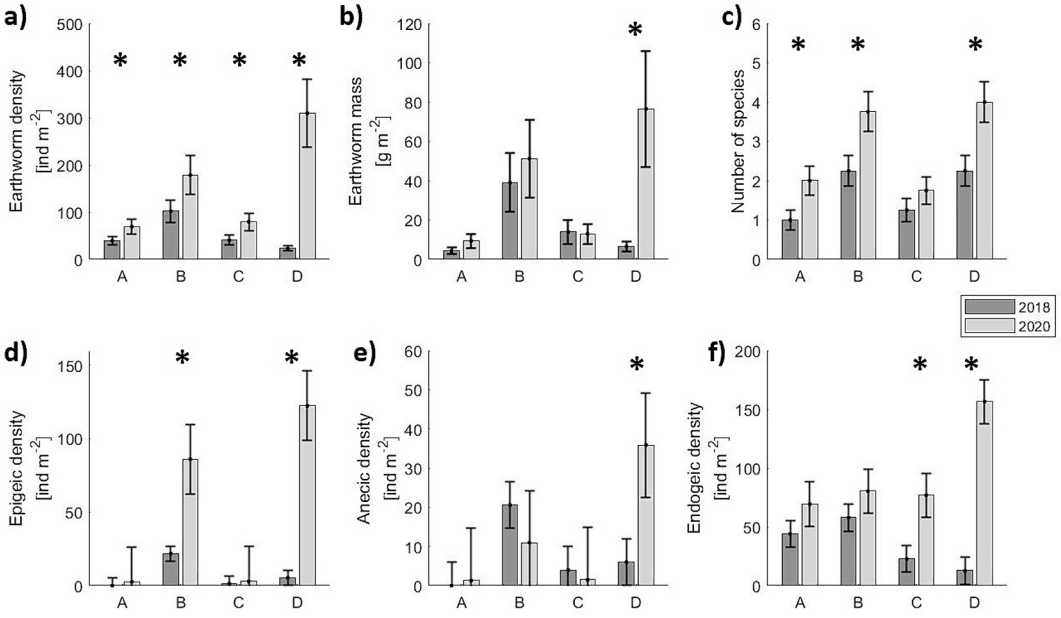


**Fig. 6.** Total earthworm density (a), their mass (b), number of species (c), and the density of Epigeic (d), Anecic (e) and Endogeic (f) species in plots A-D in October 2018 and October 2020. Error bars denote standard error and asterisks significant difference ($p < 0.05$) between years.

NEE in 2020 is likely explained by later sowing time and thus lower productivity and a high amount of decomposing crop residues in plots C and D after rapeseed cropping compared to year 2019. The results illustrate well the difficulty of maintaining SOC in annual crop cultivation in boreal soils with short growing season and low productivity.

Previously reported European NEE values are mostly lower compared to our results as the NEE has varied from −4.5 to 0.2 Mg C $ha^{-1}$ $yr^{-1}$ in Western European cereal cultivation (Abdalla et al., 2013; Vuichard et al., 2016). Liebig et al. (2022) reported NEE of 0.3 Mg C $ha^{-1}$ $yr^{-1}$ and net ecosystem carbon balance of the magnitude 1.6 Mg C $ha^{-1}$ $yr^{-1}$ for spring wheat in North Dakota which is more in line with our results. The differences are mainly due to the low productivity in Finland; the mean GP for barley of our site was 4.6 Mg C $ha^{-1}$ $yr^{-1}$ in 2020 while it varied from 9 to 19 Mg C $ha^{-1}$ $yr^{-1}$ in the above studies except in Liebig et al. (2022) who reported 6.2 Mg C $ha^{-1}$ $yr^{-1}$. In line with that, Liebig et al. (2022) observed aboveground biomass of 990 g $m^{-2}$ while ours was about 600 g $m^{-2}$ in 2022. Furthermore, carbon input by crop residues at our study site has shown a decreasing trend since 2014 (results not shown). These findings may be linked as productivity of clay soils is regulated by the ratio of clay to carbon content (Soinne et al., 2024).

As compared to soil respiration, water discharge was an insignificant route of carbon loss. Although erosion was exceptionally high due to the lack of snow cover and warm beginning of the year (even 8400 kg $ha^{-1}$ $yr^{-1}$ in plot A in 2020 compared to the long-term average of the site of 1500 (1100–2200; 95%CI) and 670 (460–970; 95%CI) kg $ha^{-1}$ $yr^{-1}$ in CT and NT, respectively (Honkanen et al., 2021)), the proportion of carbon lost in water discharge was only 1.3% of the total carbon lost from the site. The results on the rate are in line with the study of Manninen et al. (2018) and Manninen et al. (2023) who reported similar carbon loss rates in discharge at the same field site. This field represents a typical gently sloping field in southwestern Finland; in steeper slopes erosion rates are likely higher. The insignificant role of erosion in the carbon balance was partly due to the poor NEE. With a better productivity and NEE, NT with lower erosion rates could have a more positive carbon balance. Also, as compared to respired carbon, the eroded carbon may not burden the atmosphere but may deposit in the waterbodies as sediment thus acting as a sink for carbon (Van Oost et al., 2007).

### 4.2. No-tillage

We found that NT increased slightly the annual cumulative ER, summertime ER and soil respiration but decreased erosion. No significant difference was observed in productivity or yield in the study years unlike in Honkanen et al. (2021) where long-term average of yield in the same field was 17% lower in NT compared to CT. Yue et al. (2023) showed that NT reduced $CO_2$ emissions but did not affect yields at global scale while Cai et al. (2022) concluded that NT can sequester carbon in the topsoil but reduce it in deeper leading to carbon loss in the first 14 years of its application. At this site, we did not observe net carbon sequestration in NT compared to CT in the long-term, but there was an increase in particulate organic carbon in the topsoil (Honkanen et al., 2021). As Yue et al. (2023) discuss, NT is expected to reduce emissions related to organic matter decomposition due to reduction in soil aeration and breakdown of aggregates. In our experimental field, biological activity increased in NT (Fritze et al., 2024) evidently partly hampering the carbon sequestration potential. Cai et al. (2022) estimated that the benefit of NT for carbon sequestration compared to CT depends mostly on annual precipitation, initial carbon content and annual mean temperature. Based on their findings, our weather conditions and high topsoil carbon content may be related to unfavourable results on NT compared to CT.

### 4.3. Soil aggregation

Our hypothesis that aggregate breakdown in the winter diminishes SOC stabilization potential was supported by the findings on the mean aggregate size. Soil aggregate size tended to increase in the summer and decrease in the winter. Winter 2020–2021 was fairly typical as regards snow cover and soil frost and the aggregate size diminished on average by 19% with no remarkable differences between plots suggesting that even NT was not able to maintain MWD. Decrease in aggregate size in the winter is typical for boreal climatic conditions with frequent freezing and thawing (Edwards, 2013) but the same has been found also in milder climatic conditions. For instance, Bottinelli et al. (2017) reported a 37% reduction in aggregate stability during the winter period in Northwestern France. Results on MWD are thus in line with the observations that the carbon balance has been unfavourable during the experimental years.

### 4.4. Earthworms

It has been observed in clay fields of our study region that earthworms enhance the stabilization of soil aggregates (Sheehy et al., 2019) and that the density of anecic earthworms is positively associated with the fraction of large soil macroaggregates (Singh et al., 2015). In this study, the high earthworm density in the NT plots was reflected as relatively high MWD but the increase in earthworm numbers during the experiment was not specifically shown in the MWD results. Our most remarkable finding as regards earthworms was the order of magnitude increase in their mass in NT with the rapeseed break crop (plot D). The change in litter quality combined with originally abundant and diverse earthworm community caused by long-term NT likely explains the drastic increase. The nitrogen content of rapeseed is about twice that of barley, resulting in a lower C:N ratio in the residue and likely preference of its litter by earthworms (Curry and Schmidt, 2007) and subsequently enhanced growth of species populations. Increase in earthworm density can potentially also increase decomposition of organic matter in soil (Lubbers et al., 2017). The observed association between respiration measurements and earthworm abundance may relate to the findings of Nieminen et al. (2015) who reported increase in soil respiration at the living sites of the anecic *Lumbricus terrestris* both in laboratory and field experiments. In their laboratory test, 13% increase in respiration per one *L. terrestris* individual was reported. This species is abundant at parts of the studied NT plots where it contributes distinctively to crop residue incorporation (Bentley et al., 2024). Lubbers et al. (2013) reported 33% increase in $CO_2$ emissions in the presence of earthworms, and they attributed it to the ability of earthworms to mobilise protected and recalcitrant forms of organic matter. Based on these findings, it is possible that large changes in the numbers of earthworms, such as observed in plot D can have notable effects on the carbon balance.

### 4.5. Occasional ploughing

Occasional ploughing can alleviate many problems related to no-till such as phosphorus accumulation in the topsoil (Baker et al., 2017) or weed infestation but it tends to decrease SOC (Blanco-Canqui and Wortmann, 2020). When the long-term no-till plot D was ploughed once in 2018, soil carbon stratification decreased while other variables like erosion and yield were comparable to the continuous no-till plot B in 2020. Our findings about the tillage of plot D were in agreement with the study by Blanco-Canqui and Wortmann (2020) who found that although occasional tillage reduced carbon stratification, impacts on soil properties and yield are short-term (<2 years) and generally would not undo benefits of NT. One-time tillage also decreased the mean aggregate size in the topsoil of our site but increased it deeper in the soil. Topsoil carbon was partly translocated from the topsoil to deeper due to ploughing but based on the soil carbon measurements the additional organic matter was decomposed during the next two years. After tillage of the no-till plot D in July 2018, earthworm abundance was about in same level as in ploughed plots A and C. After the two following years under no-till and one year of winter rapeseed cropping, earthworm

abundance increased to even higher level than in the other NT plot B. The seemingly low impact of the single ploughing event on earthworms may have been partly due to ploughing taking place during a dry midsummer period. In such conditions large part of the population is aestivating below the ploughing depth and is not directly affected by the plough. Microbial activity was found to increase immediately after ploughing in October 2018, compared to May 2018 and also to other plots (Fritze et al., 2024).

### 4.6. Cover crop

Cover crop is a well-established practice to increase field biomass production and carbon input to soil (Poeplau and Don, 2015). The mean biomass of the most typical cover crop, Italian ryegrass, has been estimated as 2.2 Mg DM $ha^{-1}$ in boreal climatic conditions (Känkänen, 2019). Based on the typical biomass and decomposition rates from a litter bag experiment, the estimated carbon sequestration potential of cover crop is 170 kg $ha^{-1}$ $yr^{-1}$ in Finland (Heikkinen et al., 2021b), about half of the potential estimated by Poeplau and Don (2015). The growth potential of cover crops is typically low in the late autumn in boreal conditions resulting in relatively low carbon input. Cover crop biomass yield below 1 Mg $ha^{-1}$ has been estimated to lead to negligible SOC sequestration (Blanco-Canqui, 2021), and our aboveground biomass of 0.4–0.5 Mg DM $ha^{-1}$ fell clearly below that limit. This is probably the main reason for the lack of significant effects of the cover crop on plot A.

### 4.7. Uncertainty

Part of the uncertainty in the $CO_2$ results arises from the simplicity of the models as some parameters used were general values obtained from published studies. For example, soil respiration was modelled only based on soil temperature, although it can be affected also by factors such as changes in microbial community composition or activity (Yang et al., 2022) and soil moisture (Smith et al., 2018). However, annual $CO_2$ budgets can be similar between simple and more complex models even if temporal flux estimates may have large differences (Liu et al., 2022). Estimating vegetation cover using measured LAI is also problematic, as it reflects weakly the amount of active chlorophyll during cereal ripening (Gregersen et al., 2013; Delegido et al., 2015). The interpolation used in the models from the peak value of LAI to the end of August is a clear simplification, but it is in good agreement with the models and the measured GP values. The measurement results of PAR values also contain uncertainties due to possible changes in cloudiness, fogging or dirt on the plexiglass and other shading, although seemingly erroneous observations were removed in the data filtering. The plexiglass surfaces were kept as clean as possible, and fogging was kept low with a short measurement time. Model predicted soil temperature used in gap filling may cause some error, but the filled gaps were not long, and the error was mostly diurnal with low risk of significant errors in annual balances. In the carbon balance, GP, yield and residues are not necessarily in line with each other, as they are defined from different areas (GP from collars and yield from test strips with combine harvester).

## 5. Conclusions

Our results from the flux measurements show relatively high net carbon losses in boreal clay soil under annual cropping. This finding was supported by the observed changes in soil carbon concentrations and the soil aggregate size which both indicated negative development in carbon stability during the study years. Our first hypothesis that erosion is a minor component of the total carbon balance of the field ecosystem was confirmed based on the results. As relates to the second hypothesis, it was clear that NT and crop diversification did not directly affect carbon balance, but they improved diversity and activity of earthworms. The results suggested that a change in the litter quality of the crop residues, C:N ratio in this case, may have unpredictable implications in soil biological activity affecting the SOC stabilization processes. The results also supported the last hypothesis on soil aggregate breakdown during the winter diminishing SOC stabilization potential in boreal climate. The warm winter and the associated increase in biological activity during the experiment, along with poor biomass production during the measurement period probably had the most marked influence in the reduction of carbon stocks. The results highlight that changes in the carbon balance of an ecosystem due to climatic anomalies can be unexpected and rapid and can compromise the effectiveness of implemented carbon sequestration measures in field management. Therefore, it is increasingly important to implement agricultural practises with extended vegetation cover and deep-rooted species in the rotations that can alleviate the effects of climate change.

## CRediT authorship contribution statement

**Henri Honkanen:** Writing – original draft, Visualization, Validation, Software, Methodology, Investigation, Data curation, Conceptualization. **Visa Nuutinen:** Writing – review & editing, Methodology, Investigation. **Jaakko Heikkinen:** Writing – review & editing, Resources, Methodology. **Riitta Lemola:** Writing – review & editing, Resources, Data curation. **Eila Turtola:** Writing – review & editing, Conceptualization. **Janne Kaseva:** Writing – review & editing, Formal analysis. **Kristiina Lång:** Writing – original draft, Supervision, Resources, Project administration, Methodology, Funding acquisition, Conceptualization.

## Declaration of competing interest

The authors declare the following financial interests/personal relationships which may be considered as potential competing interests:

All reports financial support was provided by European Union. Henri Honkanen reports financial support was provided by Maa- ja vesitekniikan tuki ry. If there are other authors, they declare that they have no known competing financial interests or personal relationships that could have appeared to influence the work reported in this paper.

## Data availability

The datasets generated during the study are available from the corresponding author on request.

## Acknowledgements

The work was funded within the project “Crop diversification and low-input farming across Europe: from practitioners’ engagement and ecosystems services to increased revenues and value chain organization” (Diverfarming) under the European Union’s Horizon 2020 Programme for Research & Innovation [grant agreement no. 728003]. The work of H.H. was funded by Maa- ja vesitekniikan tuki ry [grant number 39754]. Natural Resources Institute Finland (Luke) was the main funding source for maintaining the research field and obtaining the long-term data. Assistance of Luke technical staff in the field and laboratory work is gratefully acknowledged.

## Appendix A. Supplementary data

Supplementary data to this article can be found online at https://doi.org/10.1016/j.geodrs.2024.e00818.

## References

Abdalla, M., Saunders, M., Hastings, A., Williams, M., Smith, P., Osborne, B., Lanigan, G., Jones, M.B., 2013. Simulating the impacts of land use in Northwest Europe on net ecosystem exchange (NEE): the role of arable ecosystems, grasslands and forest plantations in climate change mitigation. Sci. Total Environ. 465, 325–336. https://doi.org/10.1016/j.scitotenv.2012.12.030.

Amézketa, E., 1999. Soil aggregate stability: a review. J. Sustain. Agric. 14, 83–151. https://doi.org/10.1300/J064v14n02_08.
Baker, D.B., Johnson, L.T., Confesor, R.B., Crumrine, J.P., 2017. Vertical stratification of soil phosphorus as a concern for dissolved phosphorus runoff in the Lake Erie Basin. J. Environ. Qual. 46, 1287–1295. https://doi.org/10.2134/jeq2016.09.0337.
Begum, K., Zornoza, R., Farina, R., Lemola, R., Álvaro-Fuentes, J., Cerasuolo, M., 2022. Modeling soil carbon under diverse cropping systems and farming Management in Contrasting Climatic Regions in Europe. Front. Environ. Sci. 10 https://doi.org/10.3389/fenvs.2022.819162.
Bentley, P., Butt, K.R., Nuutinen, V., 2024. Two aspects of earthworm bioturbation: crop residue burial by foraging and surface casting in no-till management. Eur. J. Soil Biol. 120, 103575 https://doi.org/10.1016/j.ejsobi.2023.103575.
Blanco-Canqui, H., 2021. No-till technology has limited potential to store carbon: how can we enhance such potential? Agric. Ecosyst. Environ. 313, 107352 https://doi.org/10.1016/j.agee.2021.107352.
Blanco-Canqui, H., Wortmann, C.S., 2020. Does occasional tillage undo the ecosystem services gained with no-till? A review. Soil Tillage Res. 198, 104534 https://doi.org/10.1016/j.still.2019.104534.
Bottinelli, N., Angers, D.A., Hallaire, V., Michot, D., Guillou, C.L., Cluzeau, D., Heddadj, D., Menasseri-Aubry, S., 2017. Tillage and fertilization practices affect soil aggregate stability in a humic Cambisol of Northwest France. Soil Tillage Res. 170, 14–17. https://doi.org/10.1016/j.still.2017.02.008.
Briones, M.J.I., Schmidt, O., 2017. Conventional tillage decreases the abundance and biomass of earthworms and alters their community structure in a global meta-analysis. Glob. Chang. Biol. 23, 4396–4419. https://doi.org/10.1111/gcb.13744.
Cai, A., Han, T., Ren, T., Sanderman, J., Rui, Y., Wang, B., Smith, P., Xu, M., Li, Y., 2022. Declines in soil carbon storage under no tillage can be alleviated in the long run. Geoderma 425, 116028. https://doi.org/10.1016/j.geoderma.2022.116028.
Curry, J.P., Schmidt, O., 2007. The feeding ecology of earthworms – a review. Pedobiologia 50, 463–477. https://doi.org/10.1016/j.pedobi.2006.09.001.
Delegido, J., Verrelst, J., Rivera, J.P., Ruiz-Verdú, A., Moreno, J., 2015. Brown and green LAI mapping through spectral indices. Int. J. Appl. Earth Obs. Geoinf. 35, 350–358. https://doi.org/10.1016/j.jag.2014.10.001.
Edwards, L.M., 2013. The effects of soil freeze–thaw on soil aggregate breakdown and concomitant sediment flow in Prince Edward Island: a review. Can. J. Soil Sci. 93, 459–472. https://doi.org/10.4141/cjss2012-059.
Fritze, H., Tuomivirta, T., Orrù, L., Canfora, L., Cuartero, J., Ros, M., Pascual, J.A., Zornosa, R., Egea-Cortines, M., Lång, K., Kaseva, J., Peltoniemi, K., 2024. Effect of no-till followed by crop diversification on the soil microbiome in a boreal short cereal rotation. Biol. Fertil. Soils 60, 357–374. https://doi.org/10.1007/s00374-024-01797-x.
Gaudin, A.C.M., Tolhurst, T.N., Ker, A.P., Janovicek, K., Tortora, C., Martin, R.C., Deen, W., 2015. Increasing crop diversity mitigates weather variations and improves yield stability. PLoS One 10, 1–20. https://doi.org/10.1371/journal.pone.0113261.
Green, V.S., Stott, D.E., Cruz, J.C., Curi, N., 2007. Tillage impacts on soil biological activity and aggregation in a Brazilian Cerrado Oxisol. Soil Tillage Res. 92, 114–121. https://doi.org/10.1016/j.still.2006.01.004.
Gregersen, P.L., Culetic, A., Boschian, L., Krupinska, K., 2013. Plant senescence and crop productivity. Plant Mol. Biol. 82, 603–622. https://doi.org/10.1007/s11103-013-0013-8.
Haddaway, N.R., Hedlund, K., Jackson, L.E., Kätterer, T., Lugato, E., Thomsen, I.K., Jørgensen, H.B., Isberg, P.-E., 2017. How does tillage intensity affect soil organic carbon? A systematic review. Environ. Evid. 6, 30. https://doi.org/10.1186/s13750-017-0108-9.
Hagner, M., Pohjanlehto, I., Nuutinen, V., Setälä, H., Velmala, S., Vesterinen, E., Pennanen, T., Lemola, R., Peltoniemi, K., 2023. Impacts of long-term organic production on soil fauna in boreal dairy and cereal farming. Appl. Soil Ecol. 104944 https://doi.org/10.1016/j.apsoil.2023.104944.
Hazra, K.K., Nath, C.P., Singh, U., Praharaj, C.S., Kumar, N., Singh, S.S., Singh, N.P., 2019. Diversification of maize-wheat cropping system with legumes and integrated nutrient management increases soil aggregation and carbon sequestration. Geoderma 353, 308–319. https://doi.org/10.1016/j.geoderma.2019.06.039.
Heikkinen, J., Ketoja, E., Nuutinen, V., Regina, K., 2013. Declining trend of carbon in Finnish cropland soils in 1974–2009. Glob. Chang. Biol. 19, 1456–1469. https://doi.org/10.1111/gcb.12137.
Heikkinen, J., Keskinen, R., Regina, K., Honkanen, H., Nuutinen, V., 2021a. Estimation of carbon stocks in boreal cropland soils - methodological considerations. Eur. J. Soil Sci. 72, 934–945. https://doi.org/10.1111/ejss.13033.
Heikkinen, J., Ketoja, E., Seppänen, L., Luostarinen, S., Fritze, H., Pennanen, T., Peltoniemi, K., Velmala, S., Hanajik, P., Regina, K., 2021b. Chemical composition controls the decomposition of organic amendments and influences the microbial community structure in agricultural soils, 12, pp. 359–376. https://doi.org/10.1080/17583004.2021.1947386.
Heikkinen, J., Keskinen, R., Kostensalo, J., Nuutinen, V., 2022. Climate change induces carbon loss of arable mineral soils in boreal conditions. Glob. Chang. Biol. 28, 3960–3973. https://doi.org/10.1111/gcb.16164.
Heimsch, L., Lohila, A., Tuovinen, J.-P., Vekuri, H., Heinonsalo, J., Nevalainen, O., Korkiakoski, M., Liski, J., Laurila, T., Kulmala, L., 2021. Carbon dioxide fluxes and carbon balance of an agricultural grassland in southern Finland. Biogeosciences 18, 3467–3483. https://doi.org/10.5194/bg-18-3467-2021.
Honkanen, H., Turtola, E., Lemola, R., Heikkinen, J., Nuutinen, V., Uusitalo, R., Kaseva, J., Regina, K., 2021. Response of boreal clay soil properties and erosion to ten years of no-till management. Soil Tillage Res. 212, 105043 https://doi.org/10.1016/j.still.2021.105043.
Hyvönen, T., Huusela, E., Kuussaari, M., Niemi, M., Uusitalo, R., Nuutinen, V., 2021. Aboveground and belowground biodiversity responses to seed mixtures and mowing in a long-term set-aside experiment. Agric. Ecosyst. Environ. 322, 107656 https://doi.org/10.1016/j.agee.2021.107656.
Jat, H.S., Datta, A., Choudhary, M., Yadav, A.K., Choudhary, V., Sharma, P.C., Gathala, M.K., Jat, M.L., McDonald, A., 2019. Effects of tillage, crop establishment and diversification on soil organic carbon, aggregation, aggregate associated carbon and productivity in cereal systems of semi-arid Northwest India. Soil Tillage Res. 190, 128–138. https://doi.org/10.1016/j.still.2019.03.005.
Jensen, L.S., Salo, T., Palmason, F., Breland, T.A., Henriksen, T.M., Stenberg, B., Pedersen, A., Lundström, C., Esala, M., 2005. Influence of biochemical quality on C and N mineralisation from a broad variety of plant materials in soil. Plant Soil 273, 307–326. https://doi.org/10.1007/s11104-004-8128-y.
Jokinen, P., Pirinen, P., Kaukoranta, J.-P., Kangas, A., Alenius, P., Eriksson, P., Johansson, M., Wilkman, S., 2021. Tilastoja Suomen ilmastosta ja merestä 1991-2020. Raportteja - Rapporter - Reports 2021, 8.
Kandel, T.P., Elsgaard, L., Lærke, P.E., 2013. Measurement and modelling of CO2 flux from a drained fen peatland cultivated with reed canary grass and spring barley. GCB Bioenergy 5, 548–561. https://doi.org/10.1111/gcbb.12020.
Känkänen, H., 2019. Kerääjäkasvitoimenpiteen laadullinen toteutuminen tiloilla. In: Yli-Viikari, A. (Ed.), Maaseutuohjelman (2014–2020) ympäristöarviointi; 2019, Luonnonvara- ja biotalouden tutkimus, vol. 63, pp. 46–67.
Kladivko, E.J., Akhouri, N.M., Weesies, G., 1997. Earthworm populations and species distributions under no-till and conventional tillage in Indiana and Illinois. Soil Biol. Biochem. 29, 613–615. https://doi.org/10.1016/S0038-0717(96)00187-3.
Kremen, C., Miles, A., 2012. Ecosystem Services in Biologically Diversified versus conventional farming systems: benefits, externalities, and trade-offs. Ecol. Soc. 17 https://doi.org/10.5751/ES-05035-170440.
Kutzbach, L., Schneider, J., Sachs, T., Giebels, M., Nykänen, H., Shurpali, N.J., Martikainen, P.J., Alm, J., Wilmking, M., 2007. $CO_2$ flux determination by closed-chamber methods can be seriously biased by inappropriate application of linear regression. Biogeosciences 4, 1005–1025. https://doi.org/10.5194/bg-4-1005-2007.
Le Guillou, C., Angers, D.A., Leterme, P., Menasseri-Aubry, S., 2012. Changes during winter in water-stable aggregation due to crop residue quality. Soil Use Manag. 28, 590–595. https://doi.org/10.1111/j.1475-2743.2012.00427.x.
Liebig, M.A., Saliendra, N.Z., Archer, D.W., 2022. Carbon fluxes from a spring wheat–corn–soybean crop rotation under no-tillage management. Agrosyst. Geosci. Environ. 5, e20291 https://doi.org/10.1002/agg2.20291.
Lind, S.E., Shurpali, N.J., Peltola, O., Mammarella, I., Hyvonen, N., Maljanen, M., Raty, M., Virkajarvi, P., Martikainen, P.J., 2016. Carbon dioxide exchange of a perennial bioenergy crop cultivation on a mineral soil. Biogeosciences 13, 1255–1268. https://doi.org/10.5194/bg-13-1255-2016.
Liu, W., Fritz, C., Weideveld, S.T.J., Aben, R.C.H., van den Berg, M., Velthuis, M., 2022. Annual CO2 budget estimation from chamber-based flux measurements on intensively drained peat meadows: effect of gap-filling strategies. Front. Environ. Sci. 10 https://doi.org/10.3389/fenvs.2022.803746.
Lizarazo, C.I., Tuulos, A., Jokela, V., Mäkelä, P.S.A., 2020. Sustainable mixed cropping Systems for the Boreal-Nemoral Region. Front. Sustain. Food Syst. 4 https://doi.org/10.3389/fsufs.2020.00103.
Lloyd, J., Taylor, J.A., 1994. On the temperature dependence of soil respiration. Funct. Ecol. 8, 315–323. https://doi.org/10.2307/2389824.
Lohila, A., Aurela, M., Regina, K., Laurila, T., 2003. Soil and total ecosystem respiration in agricultural fields: effect of soil and crop type. Plant Soil 251, 303–317. https://doi.org/10.1023/A:1023004205844.
Long, S.P., Hällgren, J.-E., 1993. Measurement of CO2 assimilation by plants in the field and the laboratory. In: Hall, D.O., Scurlock, J.M.O., Bolhàr-Nordenkampf, H.R., et al. (Eds.), Photosynthesis and Production in a Changing Environment: A Field and Laboratory Manual. Springer, Netherlands, Dordrecht, pp. 129–167.
Lubbers, I.M., van Groenigen, K.J., Fonte, S.J., Six, J., Brussaard, L., van Groenigen, J.W., 2013. Greenhouse-gas emissions from soils increased by earthworms. Nat. Clim. Chang. 3, 187–194. https://doi.org/10.1038/nclimate1692.
Lubbers, I.M., Jan van Groenigen, K., Brussaard, L., van Groenigen, J.W., 2015. Reduced greenhouse gas mitigation potential of no-tillage soils through earthworm activity. Sci. Rep. 5, 13787. https://doi.org/10.1038/srep13787.
Lubbers, I.M., Pulleman, M.M., Groenigen, J.W.V., 2017. Can earthworms simultaneously enhance decomposition and stabilization of plant residue carbon? Soil Biol. Biochem. 105, 12–24. https://doi.org/10.1016/j.soilbio.2016.11.008.
Maljanen, M., Liikanen, A., Silvola, J., Martikainen, P.J., 2003. Measuring N2O emissions from organic soils by closed chamber or soil/snow N2O gradient methods. Eur. J. Soil Sci. 54, 625–631. https://doi.org/10.1046/j.1365-2389.2003.00531.x.
Manninen, N., Soinne, H., Lemola, R., Hoikkala, L., Turtola, E., 2018. Effects of agricultural land use on dissolved organic carbon and nitrogen in surface runoff and subsurface drainage. Sci. Total Environ. 618, 1519–1528. https://doi.org/10.1016/j.scitotenv.2017.09.319.
Manninen, N., Kanerva, S., Lemola, R., Turtola, E., Soinne, H., 2023. Contribution of water erosion to organic carbon and total nitrogen loads in agricultural discharge from boreal mineral soils. Sci. Total Environ. 905, 167300 https://doi.org/10.1016/j.scitotenv.2023.167300.
Manns, H.R., Martin, R.C., 2018. Cropping system yield stability in response to plant diversity and soil organic carbon in temperate ecosystems. Agroecol. Sustain. Food Syst. 42, 724–750. https://doi.org/10.1080/21683565.2017.1423529.
Meurer, K.H.E., Haddaway, N.R., Bolinder, M.A., Kätterer, T., 2018. Tillage intensity affects total SOC stocks in boreo-temperate regions only in the topsoil—a systematic review using an ESM approach. Earth Sci. Rev. 177, 613–622. https://doi.org/10.1016/j.earscirev.2017.12.015.
Minasny, B., Malone, B.P., McBratney, A.B., Angers, D.A., Arrouays, D., Chambers, A., Chaplot, V., Chen, Z.-S., Cheng, K., Das, B.S., Field, D.J., Gimona, A., Hedley, C.B., Hong, S.Y., Mandal, B., Marchant, B.P., Martin, M., McConkey, B.G., Mulder, V.L.,

O'Rourke, S., Richer-de-Forges, A.C., Odeh, I., Padarian, J., Paustian, K., Pan, G., Poggio, L., Savin, I., Stolbovoy, V., Stockmann, U., Sulaeman, Y., Tsui, C.-C., Vågen, T.-G., van Wesemael, B., Winowiecki, L., 2017. Soil carbon 4 per mille. Geoderma 292, 59–86. https://doi.org/10.1016/j.geoderma.2017.01.002.

Nieminen, M., Hurme, T., Mikola, J., Regina, K., Nuutinen, V., 2015. Impact of earthworm Lumbricus terrestris living sites on the greenhouse gas balance of no-till arable soil. Biogeosciences 12, 5481–5493. https://doi.org/10.5194/bg-12-5481-2015.

Nunes, M.R., van Es, H.M., Schindelbeck, R., Ristow, A.J., Ryan, M., 2018. No-till and cropping system diversification improve soil health and crop yield. Geoderma 328, 30–43. https://doi.org/10.1016/j.geoderma.2018.04.031.

Nuutinen, V., 2019. Earthworm sampling. In: Álvaro-Fuentes, J., Lóczy, D., Thiele-Bruhn, S., Zornoza, R. (Eds.), Handbook of Plant and Soil Analysis for Agricultural Systems. CRAI UPCT Ediciones, pp. 380–384.

Ogle, S.M., Swan, A., Paustian, K., 2012. No-till management impacts on crop productivity, carbon input and soil carbon sequestration. Agric. Ecosyst.Environ. 149, 37–49. https://doi.org/10.1016/j.agee.2011.12.010.

Ogle, S.M., Alsaker, C., Baldock, J., Bernoux, M., Breidt, F.J., McConkey, B., Regina, K., Vazquez-Amabile, G., 2019. Climate and soil characteristics determine where no-till Management can store carbon in soils and mitigate greenhouse gas emissions. Sci. Rep. 9, 11665. https://doi.org/10.1038/s41598-019-47861-7.

Olsson, L., H. Barbosa, S. Bhadwal, A. Cowie, K. Delusca, D. Flores-Renteria, K. Hermans, E. Jobbagy, W. Kurz, D. Li, D.J. Sonwa, L. Stringer, 2019: Land degradation. Climate Change and Land: An IPCC Special Report on Climate Change, Desertification, Land Degradation, Sustainable Land Management, Food Security, and Greenhouse Gas Fluxes in Terrestrial Ecosystems [P.R. Shukla, J. Skea, E. Calvo Buendia, V. Masson-Delmotte, H.-O. Pörtner, D. C. Roberts, P. Zhai, R. Slade, S. Connors, R. van Diemen, M. Ferrat, E. Haughey, S. Luz, S. Neogi, M. Pathak, J. Petzold, J. Portugal Pereira, P. Vyas, E. Huntley, K. Kissick, M. Belkacemi, J. Malley]. In press.

Palosuo, T., Heikkinen, J., Regina, K., 2015. Method for estimating soil carbon stock changes in Finnish mineral cropland and grassland soils, 6, pp. 207–220. https://doi.org/10.1080/17583004.2015.1131383.

Poeplau, C., Don, A., 2015. Carbon sequestration in agricultural soils via cultivation of cover crops – a meta-analysis. Agric. Ecosyst. Environ. 200, 33–41. https://doi.org/10.1016/j.agee.2014.10.024.

Poirier, V., Angers, D.A., Rochette, P., Whalen, J.K., 2013. Initial soil organic carbon concentration influences the short-term retention of crop-residue carbon in the fine fraction of a heavy clay soil. Biol. Fertil. Soils 49, 527–535. https://doi.org/10.1007/s00374-013-0794-6.

Raich, J.W., Rastetter, E.B., Melillo, J.M., Kicklighter, D.W., Steudler, P.A., Peterson, B. J., Grace, A.L., Moore III, B., Vorosmarty, C.J., 1991. Potential net primary productivity in South America: application of a global model. Ecol.Appl. 1, 399–429. https://doi.org/10.2307/1941899.

Saarinen, M., Heikkinen, J., Ketoja, E., Kyttä, V., Hartikainen, H., Silvennoinen, K., Valsta, L., Lång, K., 2023. Soil carbon plays a role in the climate impact of diet and its mitigation: the Finnish case. Front. Sustain. Food Syst. 7 https://doi.org/10.3389/fsufs.2023.904570.

Scharlemann, Jörn P.W., Tanner, Edmund V.J., Kapos, V., 2014. Global soil carbon: understanding and managing the largest terrestrial carbon pool. Carbon Manage. 5, 81–91. https://doi.org/10.4155/cmt.13.77.

Sheehy, J., Nuutinen, V., Six, J., Palojärvi, A., Knuutila, O., Kaseva, J., Regina, K., 2019. Earthworm Lumbricus terrestris mediated redistribution of C and N into large macroaggregate-occluded soil fractions in fine-textured no-till soils. Appl. Soil Ecol. 140, 26–34. https://doi.org/10.1016/j.apsoil.2019.04.004.

Singh, P., Heikkinen, J., Ketoja, E., Nuutinen, V., Palojärvi, A., Sheehy, J., Esala, M., Mitra, S., Alakukku, L., Regina, K., 2015. Tillage and crop residue management methods had minor effects on the stock and stabilization of topsoil carbon in a 30-year field experiment. Sci. Total Environ. 518-519, 337–344. https://doi.org/10.1016/j.scitotenv.2015.03.027.

Smith, K.A., Ball, T., Conen, F., Dobbie, K.E., Massheder, J., Rey, A., 2018. Exchange of greenhouse gases between soil and atmosphere: interactions of soil physical factors and biological processes. Eur. J. Soil Sci. 69, 10–20. https://doi.org/10.1111/ejss.12539.

Soinne, H., Hyyrynen, M., Jokubė, M., Keskinen, R., Hyväluoma, J., Pihlainen, S., Hyytiäinen, K., Miettinen, A., Rasa, K., Lemola, R., Virtanen, E., Heinonsalo, J., Heikkinen, J., 2024. High organic carbon content constricts the potential for stable organic carbon accrual in mineral agricultural soils in Finland. J. Environ. Manag. 352, 119945 https://doi.org/10.1016/j.jenvman.2023.119945.

Tamburini, G., Bommarco, R., Wanger, T.C., Kremen, C., van der Heijden, M.G.A., Liebman, M., Hallin, S., 2020. Agricultural diversification promotes multiple ecosystem services without compromising yield. Sci. Adv. 6 https://doi.org/10.1126/sciadv.aba1715 eaba1715.

Thornley, J.H., Johnson, I.R., 1990. Plant and Crop Modelling. Clarendon, Oxford, p. 669.

Turtola, E., Paajanen, A., 1995. Influence of improved subsurface drainage on phosphorus losses and nitrogen leaching from a heavy clay soil. Agric. Water Manag. 28, 295–310. https://doi.org/10.1016/0378-3774(95)01180-3.

Uusitalo, R., Lemola, R., Turtola, E., 2018. Surface and subsurface phosphorus discharge from a clay soil in a nine-year study comparing no-till and Plowing. J. Environ. Qual. 47, 1478–1486. https://doi.org/10.2134/jeq2018.06.0242.

Van Bavel, C., 1950. Mean weight-diameter of soil aggregates as a statistical index of aggregation. Proc. Soil Sci. Soc. Am. 1949 (14), 20–23.

Van Oost, K., Quine, T.A., Govers, G., De Gryze, S., Six, J., Harden, J.W., Ritchie, J.C., McCarty, G.W., Heckrath, G., Kosmas, C., Giraldez, J.V., da Silva, J.R., Marques, Merckx R., 2007. The impact of agricultural soil Erosion on the global carbon cycle. Science 318, 626–629. https://doi.org/10.1126/science.1145724.

Vuichard, N., Ciais, P., Viovy, N., Li, L., Ceschia, E., Wattenbach, M., Bernhofer, C., Emmel, C., Grünwald, T., Jans, W., Loubet, B., Wu, X., 2016. Simulating the net ecosystem CO2 exchange and its components over winter wheat cultivation sites across a large climate gradient in Europe using the ORCHIDEE-STICS generic model. Agric. Ecosyst. Environ. 226, 1–17. https://doi.org/10.1016/j.agee.2016.04.017.

Wang, X., Qi, J.-Y., Zhang, X.-Z., Li, S.-S., Latif Virk, A., Zhao, X., Xiao, X.-P., Zhang, H.-L., 2019. Effects of tillage and residue management on soil aggregates and associated carbon storage in a double paddy cropping system. Soil Tillage Res. 194, 104339 https://doi.org/10.1016/j.still.2019.104339.

Yan, J., Wang, L., Hu, Y., Tsang, Y.F., Zhang, Y., Wu, J., Fu, X., Sun, Y., 2018. Plant litter composition selects different soil microbial structures and in turn drives different litter decomposition pattern and soil carbon sequestration capability. Geoderma 319, 194–203. https://doi.org/10.1016/j.geoderma.2018.01.009.

Yang, Y., Tilman, D., Furey, G., Lehman, C., 2019. Soil carbon sequestration accelerated by restoration of grassland biodiversity. Nat. Commun. 10, 718. https://doi.org/10.1038/s41467-019-08636-w.

Yang, S., Wu, H., Wang, Z., Semenov, M.V., Ye, J., Yin, L., Wang, X., Kravchenko, I., Semenov, V., Kuzyakov, Y., Jiang, Y., Li, H., 2022. Linkages between the temperature sensitivity of soil respiration and microbial life strategy are dependent on sampling season. Soil Biol. Biochem. 172, 108758 https://doi.org/10.1016/j.soilbio.2022.108758.

Yue, K., Fornara, D.A., Hedĕnec, P., Wu, Q., Peng, Y., Peng, X., Ni, X., Wu, F., Peñuelas, J., 2023. No tillage decreases GHG emissions with no crop yield tradeoff at the global scale. Soil Tillage Res. 228, 105643 https://doi.org/10.1016/j.still.2023.105643.

Zheng, D., Hunt Jr., E.R., Running, S.W., 1993. A daily soil temperature model based on air temperature and precipitation for continental applications. Clim. Res. 2, 183–191.